FEBS Open Bio 2 (2012) 267–272

FEBS openbio

journal homepage: www.elsevier.com/locate/febsopenbio

Diacylglycerol kinase-dependent formation of phosphatidic acid molecular species during interleukin-2 activation in CTLL-2 T-lymphocytes

Satoru Mizuno[a,1], Hiromichi Sakai[a,*,1], Masafumi Saito[a], Sayaka Kado[b], Fumio Sakane[a,*]

[a] Department of Chemistry, Graduate School of Science, Chiba University, 1-33 Yayoi-cho, Inage-ku, Chiba 263-8522, Japan
[b] Chemical Analysis Center, Chiba University, 1-33 Yayoi-cho, Inage-ku, Chiba 263-8522, Japan

ARTICLE INFO

Article history:
Received 3 July 2012
Received in revised form 16 August 2012
Accepted 20 August 2012

Keywords:
Liquid chromatography/electrospray-ionization mass spectrometry
Phosphatidic acid
Diacylglycerol kinase
Interleukin-2

ABSTRACT

Although effective liquid chromatography (LC)/mass spectrometry (MS) methods enabling the separation of phospholipid molecular species have been developed, there are still problems with an intracellular signaling molecule, phosphatidic acid (PA). In this study, we optimized LC/MS conditions to improve the quantitative detection of PA molecular species from a cellular lipid mixture. Using the newly developed LC/MS method, we showed that stimulation of CTLL-2 murine T-lymphocytes by interleukin-2 (IL-2) induced a significant increase of 36:1-, 36:2-, 40:5- and 40:6-diacyl-PA. A diacylglycerol kinase (DGK) inhibitor, R59949, attenuated the increase of 36:1-, 40:5-, 40:6-diacyl-PA, suggesting that DGK IL-2-dependently and selectively generated these diacyl-PA species.

1. Introduction

Phosphatidic acid (PA) is an important intermediate in the synthesis of all phospholipids and an intracellular signaling molecule in mammalian cells. PA as a lipid second messenger performs specific tasks in a wide range of biological processes [1–3]. For, example, PA regulates phosphatidylinositol-4-phosphate-5-kinase, Ras GTPase-activating protein, Raf-1 kinase and atypical protein kinase C [3–5]. Therefore, it is essential that the cellular concentrations of PA are strictly regulated by the action of metabolic enzymes. PA as an intracellular signaling lipid is generated by phosphorylation of diacylglycerol by diacylglycerol kinase (DGK) [5–9] and hydrolysis of phosphatidylcholine by phospholipase D (PLD) [2–4].

To date, 10 mammalian DGK isozymes (α, β, γ, δ, η, κ, ε, ζ, ι and θ) have been identified, and these isozymes are subdivided into five groups according to their structural features [5–9]. Recent studies have revealed that the DGK isozymes are crucial for a wide variety of signal transduction pathways involved in development, neural and immune responses, cytoskeleton reorganization, glucose incorporation and carcinogenesis [5–10]. For example, the α-isozyme of DGK regulates the proliferation of melanoma [11] and hepatocellular carcinoma [12]. Moreover, PA produced by DGKα, which is abundantly expressed in T-lymphocytes and the thymus [13,14], is necessary for the interleukin-2 (IL-2)-induced G1-to-S transition of T-lymphocytes [15,16]. Furthermore, Jones et al. revealed that IL-2 causes an increase of PA in CTLL-2 murine T-lymphocytes that lack the IL-2-stimulating PLD activity [17,18]. These studies indicate that the DGK-dependent accumulation of PA is important for IL-2-induced T-cell proliferation. However, it remains unclear what PA molecular species are involved during IL-2-dependent T-cell proliferation.

To detect molecular species of phospholipids in cells, liquid chromatography/electrospray ionization mass spectrometry (LC/ESI-MS) is a powerful tool [19,20]. However, there are still problems with detecting PA. Because PA is a minor component of phospholipids, and because PA contains a variety of fatty acids, extensively broad PA peaks inevitably overlap with other major phospholipid peaks, causing inferior detection, quantification and reproducibility. Because of these methodology limitations, the behavior of different PA molecular species during cell stimulation is poorly understood.

In this study, we optimized LC conditions to quantitatively and reproducibly detect PA molecular species using LC/ESI-MS. To test the developed LC/ESI-MS method, we examined phospholipid mixtures from various mammalian cells including CTLL-2 T-lymphocytes, and confirmed that PA species from *m/z* 591.41 (28:0-PA) to *m/z* 759.59 (40:0-PA) were quantitatively and reproducibly detected. As a result, the PA diacyl and alkyl–acyl species profiles were found to vary between different mammalian cell lines. Moreover, we found that IL-2 stimulation caused a DGK-dependent increase of limited molecular species of PA in CTLL-2 cells.

Abbreviations: DGK, diacylglycerol kinase; DMEM, Dulbecco's modified Eagle's medium; ESI, electrospray ionization; FBS, fetal bovine serum; IL-2, interleukin-2; LC, liquid chromatography; MEF, mouse embryonic fibroblast; MS, mass spectrometry; PA, phosphatidic acid; PLD, phospholipase D.

[1] These authors contributed equally to this work.

* Corresponding author. Tel./fax: +81 43 290 3695.
E-mail address: hisakai@chiba-u.jp (H. Sakai) sakane@faculty.chiba-u.jp (F. Sakane).

2211-5463/$36.00
http://dx.doi.org/10.1016/j.fob.2012.08.006

2. Materials and methods

2.1. Cell culture

COS-7 (a simian virus 40-transformed simian kidney cell line), C2C12 (a mouse myoblast cell line) and HeLa (a human epithelial carcinoma cell line) cells as well as mouse embryonic fibroblasts (MEFs), obtained from fetal C57/BL6 mice, were maintained on 100-mm dishes in Dulbecco's modified Eagle's medium (DMEM, Wako Pure Chemicals, Tokyo, Japan) containing 10% fetal bovine serum (FBS) at 37 °C in an atmosphere with 5% CO_2. CTLL-2 (an IL-2-dependent mouse cytotoxic T-cell line) and Jurkat (a human T cell lymphoblast-like cell line) cells were maintained in 75-cm^2 flasks in RPMI-1640 medium (Wako Pure Chemicals) containing 10% FBS, 2 mM sodium pyruvate and 50 μM 2-mercaptoethanol. For CTLL-2 cell culture, 100 U/ml IL-2 (human recombinant, Wako Pure Chemicals) was added to the medium.

2.2. IL-2 stimulation

CTLL-2 cells (grown to 80% confluence) were washed twice with RPMI-1640. To starve the cells, the washed cell were incubated in serum- and IL-2-free RPMI-1640 for 90 min. The starved cells were pre-incubated with or without 25 μM DGK inhibitor R59949 (Merk Biosciences-Calbiochem, Tokyo, Japan) for 30 min and stimulated with 200 U/ml IL-2 (Wako Pure Chemicals) for 15 min.

2.3. Lipid extraction and measurement of the phospholipid amount

Cells (grown to 80% confluence) were harvested in phosphate-buffered saline. Total lipids were extracted from the cells according to the method of Bligh and Dyer [21]. An aliquot of the extracted lipids was used for measurement of the amount of inorganic phosphate in the phospholipid preparation as previously described [22].

2.4. Liquid chromatography

The extracted cellular lipids (5 μl) containing 40 pmol of the 28:0-PA internal standard (Sigma–Aldrich, Tokyo, Japan), were separated on the LC system (Accela LC Systems, Thermo Fisher Scientific, Tokyo, Japan) using a UK-Silica column (3 μm, 150 × 2.0 mm i.d., Imtakt, Kyoto, Japan). Mobile phase A consisted of chloroform/methanol/ammonia (89:10:1), and mobile phase B consisted of chloroform/methanol/ammonia/water (55:39:1:5). The gradient elution program was as follows: 30% B for 5 min, 30–60% B over 25 min, 60–70% over 5 min, followed by 70% B for 10 min. The flow rate was 0.3 ml/min, and the chromatography was performed at 25 °C.

2.5. Mass spectrometry

The LC system described above was coupled online to an Exactive Orbitrap MS (Thermo Fisher Scientific) equipped with an ESI source. The ion spray voltage was set to –5 and 5 kV in the negative and positive ion mode, respectively. The capillary temperature was set to 300 °C. The other parameters were set according to the manufacturer's recommendations. This MS system was controlled by the Xcalibur software. Individual phospholipids were measured by scanning from m/z 450 to 1100 in the negative or positive ion modes using an Orbitrap Fourier Transform MS with a resolution of 50,000. The MS peaks were identified based on their mass/charge (m/z) ratio and were presented in the form of X:Y, where X is the total number of carbon atoms and Y is the total number of double bonds in both acyl chains of the phospholipid.

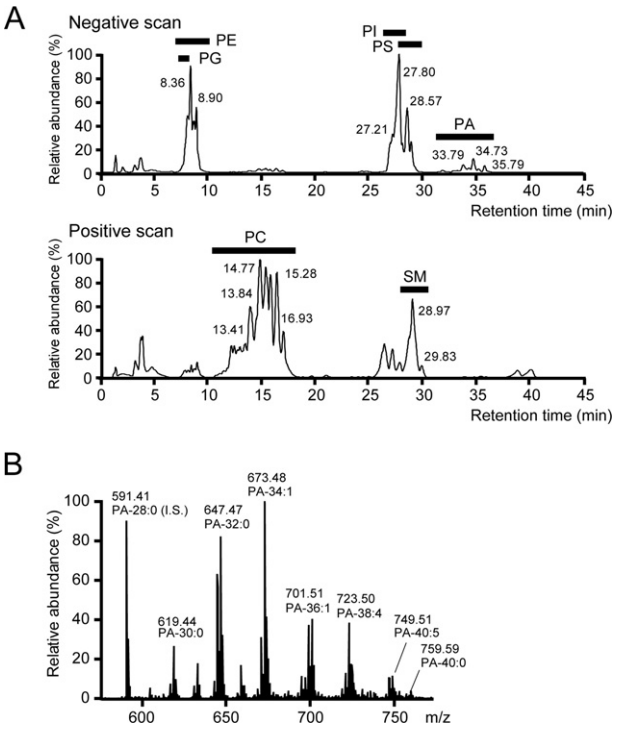

Fig. 1. Separation of PA and identification of PA molecular species by LC/ESI-MS. (A) PAs in MEFs were separated from other phospholipids by the Accela LC System using a UK-Silica column with mobile phases containing 0.28% ammonia. (B) Negative-ion ESI/MS spectra with PA species from m/z 591.41 (28:0-PA) to m/z 759.59 (40:0-PA) were identified. *Abbreviations*:I.S., internal standard, PA, phosphatidic acid; PC, phosphatidylcholine; PE, phosphatidylethanolamine; PG, phosphatidylglycerol; PI, phosphatidylinositol; PS, phosphatidylserine; SM, sphingomyelin.

2.6. Statistics

All LC/ESI-MS data were normalized based on the inorganic phosphate content and the intensity of the internal standard and were represented as the mean ± SD. Statistical analysis was performed by the two-tailed t-test.

3. Results

3.1. Improvement of PA species detection using LC/ESI-MS

Pettitt et al. and Shui et al. reported that PA molecular species can be separated from total lipid extracts of eukaryotic cells using silica column LC/MS [23,24]. We attempted to separate PA species from total lipids extracted from MEFs according to the previously reported LC conditions. However, because PA elutes relatively close to phosphatidylcholine and sphingomyelin using these conditions, PA often overlapped with the major phospholipids (Suppl. Fig. 1), causing inferior reproducibility. Thus, we optimized the LC conditions to establish an improved PA separation. We found that the PA peaks were completely separated from other phospholipid species when mobile phases A and B were changed to chloroform/methanol/ammonia (89:10:1) and chloroform/methanol/ammonia/water (55:39:1:5), respectively (Fig. 1A).

The detected diacyl- and alkyl–acyl-PA species were listed in Tables 1 and 2 and all had mass accuracies less than ±6 ppm. In addition, the representative MS spectra pattern of the PA species from m/z 591.41 (28:0-PA, internal standard) to m/z 759.59 (40:0-PA) was shown in Fig. 1B. Moreover, we tested the reproducibility of quantitative detection of cellular diacyl-PA species in MEFs. The repeated

Table 1
Identification of diacyl-PA species in MEFs.

Species	Theoretical m/z	Measured m/z	Mass error[a] (ppm)
28:0 (I.S.[b])	591.4022	591.4052	5.0
30:2	615.4022	615.4049	4.3
30:1	617.4179	617.4209	4.9
30:0	619.4335	619.4364	4.6
32:3	641.4179	641.4195	2.5
32:2	643.4335	643.4371	5.6
32:1	645.4492	645.4524	5.0
32:0	647.4648	647.4674	4.0
34:4	667.4335	667.4352	2.5
34:3	669.4492	669.4516	3.6
34:2	671.4648	671.4683	5.2
34:1	673.4804	673.4831	3.9
34:0	675.4961	675.4965	0.6
36:5	693.4492	693.4517	3.7
36:4	695.4648	695.4673	3.6
36:3	697.4804	697.4836	4.5
36:2	699.4961	699.4991	4.3
36:1	701.5117	701.5138	3.0
36:0	703.5274	703.5265	−1.2
38:7	717.4492	717.4523	4.4
38:6	719.4648	719.4682	4.7
38:5	721.4804	721.4836	4.4
38:4	723.4961	723.4992	4.3
38:3	725.5117	725.5139	3.0
38:2	727.5274	727.5301	3.8
38:1	729.5430	729.5461	4.2
38:0	731.5586	731.5615	3.9
40:6	747.4961	747.4994	4.4
40:5	749.5117	749.5144	3.6
40:4	751.5274	751.5254	−2.6
40:1	757.5743	757.5773	4.0
40:0	759.5899	759.5927	3.7

[a] Difference between theoretical m/z and measured m/z.
[b] I.S., internal standard.

Table 2
Identification of alkyl – acyl-PA species in MEFs.

Species	Theoretical m/z	Measured m/z	Mass error[a] (ppm)
30:1	603.4386	603.4417	5.1
30:0	605.4543	605.4575	5.4
32:3	627.4386	627.4399	2.1
32:1	631.4699	631.4734	5.6
32:0	633.4855	633.4890	5.5
34:4	653.4543	653.4558	2.4
34:3	655.4699	655.4721	3.4
34:2	657.4855	657.4890	5.3
34:1	659.5012	659.5046	5.2
34:0	661.5168	661.5198	4.5
36:6	677.4543	677.4571	4.2
36:5	679.4699	679.4730	4.6
36:4	681.4855	681.4885	4.4
36:3	683.5012	683.5050	5.6
36:2	685.5168	685.5203	5.1
36:1	687.5325	687.5360	5.2
36:0	689.5481	689.5508	3.9
38:7	703.4699	703.4731	4.6
38:6	705.4855	705.4892	5.2
38:5	707.5012	707.5050	5.4
38:1	715.5637	715.5643	0.8
40:2	741.5794	741.5824	4.1
40:1	743.5950	743.5985	4.7
40:0	745.6107	745.6142	4.8

[a] Difference between theoretical m/z and measured m/z.

experiments between periods on a given study day (within-day reproducibility) and between the three study days (between-day reproducibility) exhibited excellent reproducibility (Suppl. Fig. 2). These results indicate that our LC/ESI-MS method provided reproducible and quantitative detection of cellular PA species profiles.

To determine recovery rate, a mixture of standard 28:0-, 36:2-, 38:4-PA (80 pmol of each) were added to MEFs before and after the extraction process. The calculated recovery rates were 74.4 ± 10.1% for a mixture of 28:0-, 36:2 and 38:4-PA. Moreover, we established standard curves using different amounts (0.59–146 pmol) of standard 28:0-PA and 38:4-PA. Both 28:0- and 38:4-PA displayed linear curves in the high and low amount range tested and the slopes of the linear curves of 28:0-PA and 38:4-PA were very similar (Fig. 2). In addition, standard curves using various amount of both 28:0- and 38:4-PA showed good linearity at the high (9.50–146 pmol, $r > 0.995$) and low ranges (0.59–9.50, $r > 0.985$), suggesting that the length of fatty acyl chains and double bond did not affect ionization efficiency significantly.

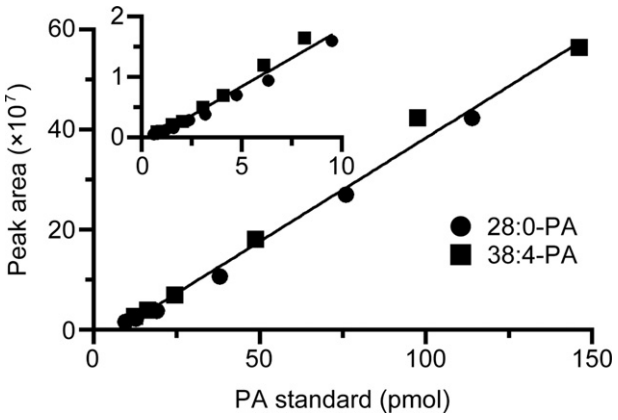

Fig. 2. Standard curves obtained with the LC/ESI-MS method and PA standards (28:0- and 38:4-PA). The main panel shows the high-range standard curve (9.50–146 pmol; $y = 4.14 \times 10^6 x - 29.74 \times 10^6$, $r = 0.995$) and the inset exhibits the low-range standard curve (0.59–9.50 pmol; $y = 1.90 \times 10^6 x - 1.05 \times 10^6$, $r = 0.985$).

3.2. MS profiles of PA species in various mammalian cells

To test the new LC/ESI-MS method, we detected and quantitated PA molecular species in various mammalian cells. The primary common components in adherent cells (COS7, C2C12 and HeLa cells (Suppl. Fig. 3) and MEFs (Fig. 3A)) were diacyl-PA species with saturated and mono- and/or di-unsaturated fatty acids (32:1-, 34:1-, 34:2-, 36:1- and 36:2-PA). In addition, several PA species varied in abundance in the different cell lines: 30:0- and 32:0-PA, which contain only saturated fatty acids, were abundant in MEFs; 40:5-PA in COS7 cells; 40:6-PA in C2C12 cells; 38:4- and 40:3-PA in HeLa cells. For non-adherent T cell-derived cell lines (*i.e.*, CTLL-2 and Jurkat), 32:0-, 34:1-, 36:1-, 36:2-, 40:5- and 40:6-PA were abundant in CTLL-2 cells (Fig. 3C). Compared with the adherent cell lines, 40:5- and 40:6-PA, containing poly-unsaturated fatty acids, were particularly enriched in the T-cells. Interestingly, PAs in Jurkat cells mainly consisted of 34:0-, 34:1-, 34:2-, 36:1-, 36:2- and 36:3-PA, comprising >95% of the total PAs (Fig. 3E). These results indicated that the PA species differed moderately in the different adherent cell lines and the CTLL-2 cells. Interestingly, the Jurkat cells had a unique PA species profile.

We next identified alkyl–acyl-PA species in CTLL-2 cells. The total amount of alkyl–acyl-PA species was 12.5 ± 0.4% of the total amount of diacyl-PA species. As shown in Fig. 3D, 32:0-, 34:1-, 34:0- and 38:5-alkyl–acyl-PA were the major components. The results indicated that the major alkyl–acyl-PA species differed from the major diacyl-PA species (Fig. 3C and D). Because alkyl–acyl-PAs in Jurkat cells were only present in a trace amount (0.2 ± 0.1% of total diacyl-PA), we could not quantitatively detect those lipids. Alkyl–acyl-PA species in MEFs (8.6 ± 0.4% of total diacyl-PA), C2C12 cells (3.0 ± 0.1% of total diacyl-PA) and HeLa cells (16.2 ± 0.1% of total diacyl-PA) exhibited essential the same profiles as those of CTLL-2 cells (Fig. 3 and Suppl.

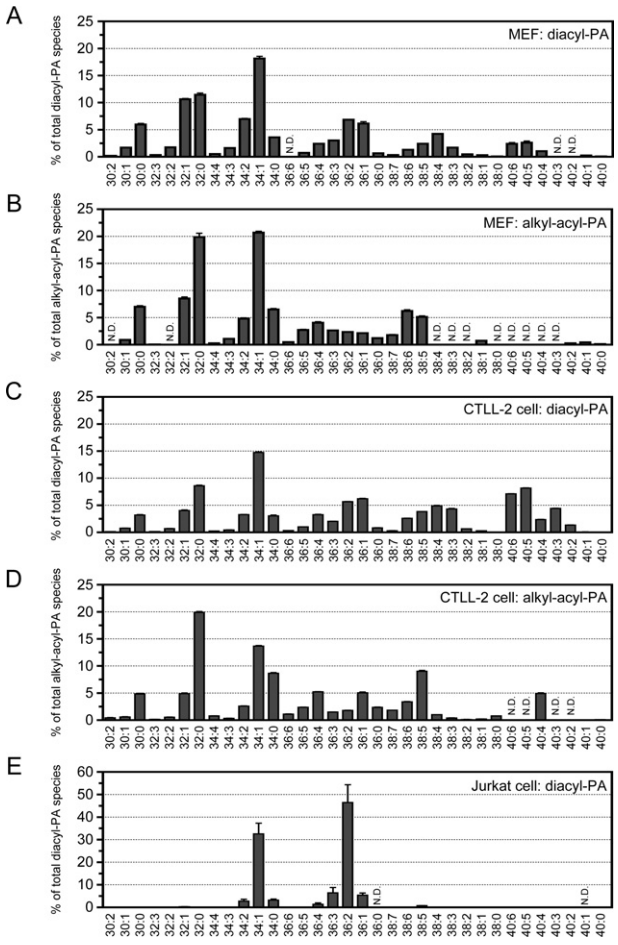

Fig. 3. Profiles of PA species in mammalian cells (MEFs, and CTLL-2 cells and Jurkat cells). (A, C and E) The molecular species composition of diacyl-PAs in MEFs (A), CTLL-2 cells (C) and Jurkat cells (E). (B and D) The molecular species composition of alkyl–acyl-PAs in MEFs (B) and CTLL-2 cells (D). The values are presented as the mean ± SD ($n = 3$). N.D., not detected.

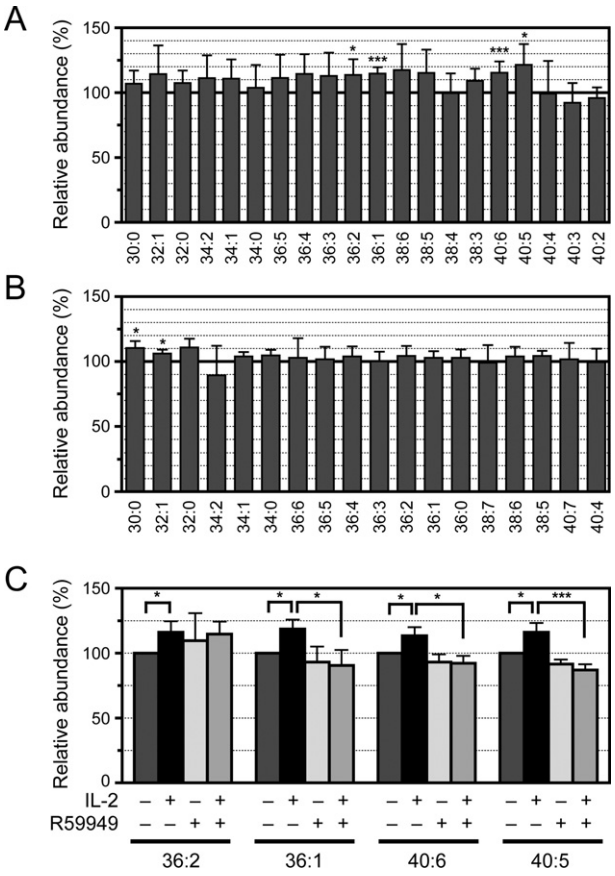

Fig. 4. Effects of IL-2 and the DGK inhibitor, R59949, on the PA species level in CTLL-2 cells. (A and B) The amount of diacyl-PA species (A) and alkyl–acyl-PA species (B) in IL-2-stimulated or IL-2-unstimulated CTLL-2 cells were measured. The results are presented as the percentage of the value of PA species in control cells without IL-2 treatment. PA species with >1% of the total diacyl-PA species or alkyl–acyl-PA species content are shown (Fig. 2C and D). The values are presented as the mean ± SD ($n = 5$). (C) The amount of diacyl-PA species in IL-2-stimulated or IL-2-unstimulated CTLL2 cells with or without R59949 treatment was measured. The results are presented as the percentage of the value of PA species in control cells without IL-2 stimulation or R59949 treatment. The values are presented as the mean ± SD ($n = 3$). * $p < 0.05$; *** $p < 0.005$.

Fig. 3). Intriguingly, 38:7-, 36:6-, 38:2-, 40:4- and 40:3-alkyl–acyl-PA species were enriched in COS7 cells (Suppl. Fig. 3). In summary, we concluded that the diacyl and alkyl–acyl-PA profiles are quite different among different mammalian cell lines, and that our new LC/ESI-MS method reproducibly and quantitatively detected cellular PA species profiles.

3.3. Alteration of PA species levels in CTLL-2 cells by IL-2 stimulation

IL-2 causes an increase in PA [18]. Hence, we analyzed the induction of PA species by IL-2 stimulation in CTLL-2 cells using our new LC/ESI-MS method. As shown in Fig. 4A, IL-2 stimulation for 15 min broadly increased diacyl-PA-species, in particular, 36:2-, 36:1-, 40:5- and 40:6-diacyl-PA with statistical significance. Interestingly, IL-2 did not augment the amount of 38:4-PA (1-stearoyl-2-arachidonoyl-PA), which is generated from phosphatidylinositol turnover-derived 38:4-diacylglycerol. In addition, the stimulation also failed to alter the amounts of 34:0-, 40:4-, 40:3- and 40:2-PA. We were unable to detect any significant change in alkyl–acyl-PA species (<10% change) (Fig. 4B).

DGK is activated by IL-2 stimulation and is involved in IL-2-dependent T-cell proliferation [15,16]. We therefore investigated whether the statistically significant, IL-2-induced increases of 36:2, 36:1-, 40:5- and 40:6-PA were inhibited by a DGK inhibitor, R59949. R59949 attenuated the IL-2-dependent increases of 36:1-, 40:5- and 40:6-PA in CTLL-2 cells, whereas the inhibitor did not affect the increase of 36:2-PA (Fig. 4C). These results strongly suggested that R59949-sensitive DGK in CTLL-2 cells selectively generated 36:1-, 40:5- and 40:6-PA in an IL-2-dependent manner. Moreover, the increases of 30:0-, 32:1-, 36:5-, 36:4- and 36:3-diacyl-PA as well as 30:0-, 32:1- and 32:2-alkyl–acyl-PA were inhibited by R59949, whereas those of 34:2, 36:3, 38:6 and 38:5 were not inhibited (data not shown). Therefore, these R59949-inhibited PA species are likely generated by the R59949-sensitive DGK.

4. Discussion

Because PA eluted relatively close to phosphatidylcholine and/or sphingomyelin using previously established methods [23,24], PA often overlapped with these major phospholipids, causing inferior reproducibility. For this study, we thus optimized the LC conditions, including the mobile phase composition and the solvent program to establish a new LC/ESI-MS system suitable for analysis of PA molecular species (Fig. 1). The LC/ESI-MS system stably and reproducibly detected PA species from various mammalian cell lines (Figs. 2 and 3 and Suppl. Fig. 3). Using the developed method, we obtained the following information.

PAs in various mammalian cell lines (MEFs and COS7, C2C12, HeLa,

CTLL-2 and Jurkat cells) contained different diacyl and alkyl–acyl species profiles (Fig. 3). In particular, Jurkat T-cells contained quite different PA profiles compared with other cell lines. Diacyl-PAs in Jurkat cells mainly consisted of 34:0-, 34:1-, 34:2-, 36:1-, 36:2- and 36:3-PA, comprising >95% of the total diacyl-PAs (Fig. 3E). The reason for the different profiles is unknown. Jeong et al. reported that cancer cells and normal cells have different profiles of PAs and individual phospholipids [25]. PA metabolism may therefore be abnormal in Jurkat T-cell lymphoma cells. However, because HeLa cells are also derived from cancer cells (human epithelial carcinoma), the difference in the PA species profile may depend on the nature of the cancer.

Although IL-2 causes an increase in PA in CTLL-2 cells, the molecular species of PA have not yet been elucidated. In this study, we found for the first time that IL-2 stimulation enhanced the production of a broad range of diacyl-PA species, in particular 36:2-, 36:1-, 40:5- and 40:6-diacyl-PA with statistical significance (Fig. 4A). Notably, IL-2 did not increase an amount of 38:4-PA (1-stearoyl-2-arachidonoyl-PA) produced from phosphatidylinositol turnover-derived 38:4-diacylglycerol. The results indicate that the IL-2-dependent PA generation occurs in a phosphatidylinositol turnover-independent fashion. Therefore, the substrate diacylglycerol is likely supplied from an unknown source rather than from phosphatidylinositol turnover.

Jones et al. reported that IL-2 mainly stimulates the formation of alkyl–acyl-PAs, but not diacyl-PAs [18]. However, we detected mainly an increase in the diacyl-PA species level. The cause of this discrepancy is unknown at present but may be due to the difference in the employed methods, *e.g.*, MS analysis by gas chromatography/MS in Ref. [18] and LC/ESI-MS in the present study.

Of the IL-2-sensitive diacyl-PA species (36:2-, 36:1-, 40:5- and 40:6-diacyl-PA) that showed a statistically significant increase (Fig. 4A), only the increase of 36:1-, 40:5- and 40:6-PA was attenuated by the DGK inhibitor, R59949 (Fig. 4C), indicating that these PA species were produced by the IL-2-activated, R59949-sensitive DGK. Moreover, 30:0-, 32:1-, 36:5-, 36:4- and 36:3-diacyl-PA as well as 30:0-, 32:1- and 32:2-alkyl–acyl-PA were also sensitive to R59949 and may thus be products of DGK. R59949 was reported to inhibit calcium-dependent, type I DGK isozymes (α, β and γ) *in vitro* [26]. We also observed that, of the 10 DGK isozymes, this inhibitor strongly inhibited DGKα and γ *in vitro* (Sato and Sakane, unpublished work). Moreover, we confirmed that DGKα but not DGKβ or γ was highly expressed in CTLL-2 cells (data not shown). DGKα is activated in response to IL-2 stimulation in CTLL-2 cells [17]. However, this cell line lacks IL-2-induced PLD activity [17]. Hence, DGKα is likely mainly responsible for the IL-2-dependent production of PA species. Moreover, it is possible that the R59949-insensitive increase of 36:2-PA is catalyzed by R59949-insensitive DGK or other enzyme(s), including a trace amount of IL-2-responsive PLD. A conclusive determination of the IL-2-responsible DGK isozyme(s) was not the purpose of this study. We are currently characterizing DGK isozymes by performing several experiments, including DGK isozyme-specific knockdowns, and would like to report our results elsewhere in a future work.

In addition to PLD [2–4], DGK appears to participate in various pathophysiological events by modulating PA levels [5–10]. However, the cellular behavior of PA species, in particular the influence of receptor stimulation on the PA level, has not been clarified, mainly because of methodological limitations. We developed a new LC/ESI-MS method using a silica column LC and mobile phases containing high concentrations of ammonia. The method developed in this study will be advantageous for pathophysiological and lipidomics studies of cellular responses.

Acknowledgments

This work was supported in part by grants from the Ministry of Education, Culture, Sports, Science and Technology of Japan, the Japan Science and Technology Agency, the Naito Foundation, the Hamaguchi Foundation for the Advancement of Biochemistry, the Daiichi-Sankyo Foundation of Life Science, the Terumo Life Science Foundation, the Futaba Electronic Memorial Foundation, the Daiwa Securities Health Foundation, the Ono Medical Research Foundation and the Japan Foundation for Applied Enzymology.

Supplementary data

Supplementary data associated with this article can be found, in the online version, at doi:10.1016/j.fob.2012.08.006.

References

[1] English D. (1996) Phosphatidic acid: a lipid messenger involved in intracellular and extracellular signalling. Cell. Signal. 8, 341–347.
[2] Exton J.H. (1994) Phosphatidylcholine breakdown and signal transduction. Biochim. Biophys. Acta. 1212, 26–42.
[3] Hodgkin M.N., Pettitt T.R., Martin A., Michell R.H., Pemberton A.J., Wakelam M.J. (1998) Diacylglycerols and phosphatidates: which molecular species are intracellular messengers. Trends Biochem. Sci. 23, 200–204.
[4] Jang J.H., Lee C.S., Hwang D., Ryu S.H. (2012) Understanding of the roles of phospholipase D and phosphatidic acid through their binding partners. Prog. Lipid Res. 51, 71–81.
[5] Sakane F., Imai S., Kai M., Yasuda S., Kanoh H. (2007) Diacylglycerol kinases: why so many of them. Biochim. Biophys. Acta. 1771, 793–806.
[6] Goto K., Hozumi Y., Kondo H. (2006) Diacylglycerol, phosphatidic acid, and the converting enzyme, diacylglycerol kinase, in the nucleus. Biochim. Biophys. Acta. 1761, 535–541.
[7] Merida I., Avila-Flores A., Merino E. (2008) Diacylglycerol kinases: at the hub of cell signalling. Biochem. J. 409, 1–18.
[8] Shulga Y.V., Topham M.K., Epand R.M. (2011) Regulation and functions of diacylglycerol kinases. Chem. Rev. 111, 6186–6208.
[9] van Blitterswijk W.J., Houssa B. (2000) Properties and functions of diacylglycerol kinases. Cell. Signal. 12, 595–605.
[10] Sakane F., Imai S., Kai M., Yasuda S., Kanoh H. (2008) Diacylglycerol kinases as emerging potential drug targets for a variety of diseases. Curr. Drug Targets. 9, 626–640.
[11] Yanagisawa K. (2007) Diacylglycerol kinase α suppresses tumor necrosis factor-α-induced apoptosis of human melanoma cells through NF-κB activation. Biochim. Biophys. Acta. 1771, 462–474.
[12] Takeishi K. (2012) Diacylglycerol kinase alpha enhances hepatocellular carcinoma progression by activation of Ras–Raf–MEK–ERK pathway. J. Hepatol. 57, 77–83.
[13] Sakane F., Yamada K., Kanoh H., Yokoyama C., Tanabe T. (1990) Porcine diacylglycerol kinase sequence has zinc finger and E–F hand motifs. Nature. 344, 345–348.
[14] Yamada K., Sakane F., Kanoh H. (1989) Immunoquantitation of 80 kDa diacylglycerol kinase in pig and human lymphocytes and several other cells. FEBS Lett. 244, 402–406.
[15] Flores I., Casaseca T., Martinez-A C., Kanoh H., Merida I. (1996) Phosphatidic acid generation through interleukin 2 (IL-2)-induced α-diacylglycerol kinase activation is an essential step in IL-2-mediated lymphocyte proliferation. J. Biol. Chem. 271, 10334–10340.
[16] Flores I., Jones D.R., Cipres A., Diaz-Flores E., Sanjuan M.A., Merida I. (1999) Diacylglycerol kinase inhibition prevents IL-2-induced G1 to S transition through a phosphatidylinositol-3 kinase-independent mechanism. J. Immunol. 163, 708–714.
[17] Jones D.R., Flores I., Diaz E., Martinez-A C., Merida I. (1998) Interleukin-2 stimulates a late increase in phosphatidic acid production in the absence of phosphlipase D activation. FEBS Lett. 433, 23–27.
[18] Jones D.R., Pettitt T.R., Sanjuan M.A., Merida I., Wakelam M.J. (1999) Interleukin-2 causes an increase in saturated/monounsaturated phosphatidic acid derived from 1,2-diacylglycerol and 1-O-alkyl-2-acylglycerol. J. Biol. Chem. 274, 16846–16852.
[19] Pulfer M., Murphy R.C. (2003) Electrospray mass spectrometry of phospholipids. Mass Spectrom. Rev. 22, 332–364.
[20] Houjou T., Yamatani K., Imagawa M., Shimizu T., Taguchi R. (2005) A shotgun tandem mass spectrometric analysis of phospholipids with normal-phase and/or reverse-phase liquid chromatography/electrospray ionization mass spectrometry. Rapid Commun. Mass Spectrom. 19, 654–666.
[21] Bligh E.G., Dyer W.J. (1959) A rapid method of total lipid extraction and purification. Can. J. Biochem. Physiol. 37, 911–917.
[22] Rouser G., Siakotos A.N., Fleischer S. (1966) Quantitative analysis of phospholipids by thin-layer chromatography and phosphorus analysis of spots. Lipids. 1, 85–86.

[23] Pettitt T.R., McDermott M., Saqib K.M., Shimwell N., Wakelam M.J. (2001) Phospholipase D1b and D2a generate structurally identical phosphatidic acid species in mammalian cells. Biochem. J. 360, 707–715.
[24] Shui G., Guan X.L., Gopalakrishnan P., Xue Y., Goh J.S., Yang H. (2010) Characterization of substrate preference for Slc1p and Cst26p in *Saccharomyces cerevisiae* using lipidomic approaches and an LPAAT activity assay. PLoS one. 5, e11956.
[25] Jeong R.U., Lim S., Kim M.O., Moon M.H. (2011) Effect of D-allose on prostate cancer cell lines: phospholipid profiling by nanoflow liquid chromatography-tandem mass spectrometry. Anal. Bioanal. Chem. 401, 689–698.
[26] Jiang Y., Sakane F., Kanoh H., Walsh J.P. (2000) Selectivity of the diacylglycerol kinase inhibitor 3–2-(4-[bis-(4-fluorophenyl)methylene]-1-piperidinyl)ethyl-2,3-dihydro-2-thioxo-4(1H)quinazolinone (R59949) among diacylglycerol kinase subtypes. Biochem. Pharmacol. 59, 763–772.